Langmuir

ARTICLE

pubs.acs.org/Langmuir

Bioconjugation of Protein-Repellent Zwitterionic Polymer Brushes Grafted from Silicon Nitride

Ai T. Nguyen,[†] Jacob Baggerman,[‡] Jos M. J. Paulusse,[†] Han Zuilhof,[*,†] and Cees J. M. van Rijn[*,†,‡]

[†]Laboratory of Organic Chemistry, Wageningen University, Dreijenplein 8, 6703 HB Wageningen, The Netherlands

[‡]Aquamarijn Micro Filtration B.V., Berkelkade 11, 7201 JE Zutphen, The Netherlands

Supporting Information

ABSTRACT: A new method for attaching antibodies to protein-repellent zwitterionic polymer brushes aimed at recognizing microorganisms while preventing the nonspecific adsorption of proteins is presented. The poly(sulfobetaine methacrylate) (SBMA) brushes were grafted from α-bromo isobutyryl initiator-functionalized silicon nitride (Si_xN_4, $x \geq 3$) surfaces via controlled atom-transfer radical polymerization (ATRP). A trifunctional tris(2-aminoethyl)amine linker was reacted with the terminal alkylbromide of polySBMA chains. *N*-Hydroxysuccinimide (NHS) functionalization was achieved by reacting the resultant amine-terminated polySBMA brush with bifunctional suberic acid bis(*N*-hydroxysuccinimide ester). Anti-*Salmonella* antibodies were subsequently immobilized onto polySBMA-grafted Si_xN_4 surfaces through these NHS linkers. The protein-repellent properties of the polySBMA-grafted surface after antibody attachment were evaluated by exposing the surfaces to Alexa Fluor 488-labeled fibrinogen (FIB) solution (0.1 $g \cdot L^{-1}$) for 1 h at room temperature. Confocal laser scanning microscopy (CLSM) images revealed the minimal adsorption of FIB onto the antibody-coated polySBMA in comparison with that of antibody-coated epoxide monolayers and also bare Si_xN_4 surfaces. Subsequently, the interaction of antibodies immobilized onto polySBMA with SYTO9-stained *Salmonella* solution without using blocking solution was examined by CLSM. The fluorescent images showed that antibody-coated polySBMA efficiently captured *Salmonella* with only low background noise as compared to antibody-coated monolayers lacking the polymer brush. Finally, the antibody-coated polySBMA surfaces were exposed to a mixture of Alexa Fluor 647-labeled FIB and *Salmonella* without the prior use of a blocking solution to evaluate the ability of the surfaces to capture bacteria while simultaneously repelling proteins. The fluorescent images showed the capture of *Salmonella* with no adsorption of FIB as compared to antibody-coated epoxide surfaces, demonstrating the potential of the zwitterionic layer in preventing the nonspecific adsorption of the proteins during the detection of bacteria in complex matrices.

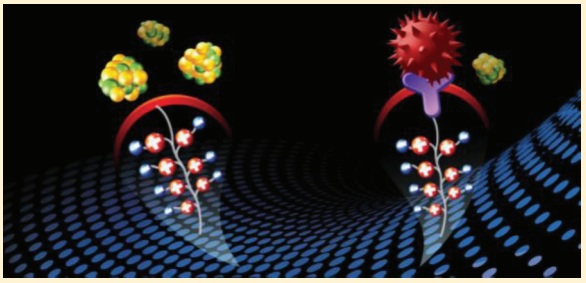

1. INTRODUCTION

There is a great need to develop novel biosensing materials that enable the attachment of ultralow fouling and biofunctionalizable surface coatings, which can be used for the highly sensitive detection of analytes directly from complex matrices. The pioneering of antibody-based biosensors[1] has had a tremendous impact on the development of new biosensing devices, such as planar microarrays,[2] bead-based microarrays,[3] and protein biochips.[4] Despite major advances in the field of diagnostics, several shortcomings still remain, such as interfering background noise as a result of the nonspecific adsorption of unwanted species within biological samples.[5−7] This may lead to a misinterpretation of results and limits the precision of diagnostic instruments.[8−11] As a consequence, the use of blocking agents, such as protein bovine serum albumin, Tween-20, or sodium dodecyl sulfate, is considered to be a prerequisite step in shielding the reactive surface sites so as to minimize the nonspecific adsorption of proteins.[5,7,12] Achieving sufficiently low degrees of nonspecific binding in sensing devices is therefore of pivotal importance for highly selective microbial detection directly from crude biological samples.[7]

Several studies have focused on the incorporation of protein-repellent coatings into biorecognition layers to improve selective capture.[13−17] For example, the immobilization of horseradish peroxidase and chicken immunoglobulin proteins on poly(ethylene oxide) films grafted from silicon chips via NHS moieties attached to polymer chain ends was studied by Feng and co-workers.[15] Although poly(ethylene oxide) is well known for its protein resistance and biocompatibility, the polymer is also found to auto-oxidize in aqueous solution, resulting in the significant cleavage of ethylene oxide units, which deteriorates the protein-repellent performance of poly(ethylene oxide) over time.[18] In addition, poly(ethylene oxide) loses much of its protein resistance at 37 °C (body temperature), which limits

Received: August 11, 2011
Revised: October 22, 2011
Published: November 07, 2011

Scheme 1. Procedure for the Attachment of Anti-*Salmonella* Antibodies to polySBMA-Coated Si_xN_4 Surfaces

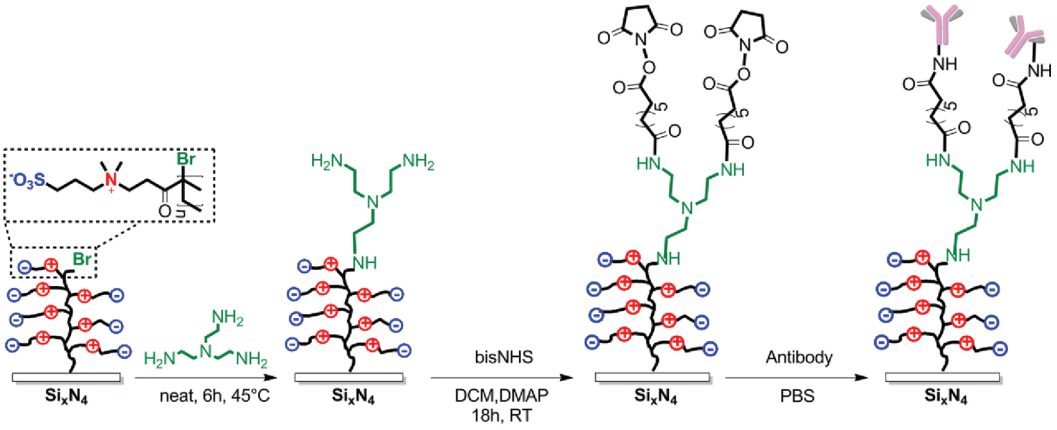

its application to in vivo biosensors, thereby influencing device sensitivity.[19,20]

As an alternative to poly(ethylene oxide), zwitterionic polymer brushes were identified as an outstanding protein-repellent material owing to the hydration layer formed via ionic solvation surrounding adjacent positive and negative charges within zwitterionic brushes.[21−28] The immobilization of antibodies specifically for cancer biomarkers on the zwitterionic poly(carboxy betaine) films was achieved by the activation of the carboxylic acid groups with NHS moieties, as reported by Brault et al.[13] and Gao et al.[14] The modified surfaces obtained by this approach show excellent results in recognizing cancer biomarkers from undiluted blood samples. Another approach to biofunctionalizing zwitterionic polymers was introduced by Kitano and coworkers in which a second polymer-containing NHS moiety was grown on top of the zwitterionic polymer brushes.[29] This approach produces a dense layer of NHS moieties, which effects a high surface coverage of a sugar-binding protein, concanavalin A. The protein adsorption of bovine serum albumin on concanavalin-modified surfaces remained low; however, the modified surfaces became less hydrophilic. This reduced hydrophilicity might be caused by the additional dense layer of NHS moieties that may shield the zwitterionic polymer beneath.

A major disadvantage of these approaches is the limited hydrolytic stability of the Si−O−Si−C[15,29] and Si−O−C[13,14] linkages through which the coatings are attached, as reported by Menawat et al.[30,31] This may result in the detachment of the protein-repellent polymer coating and consequently the cleavage of the immobilized biomolecules, keeping long-term application out of reach.

Most antibody-based microarrays are based on planar substrates allowing highly selective multiplex detection.[4,7,32] However, planar surfaces are often limited by mass transfer or the diffusion of cells toward the surface as well as the adequate affinity of the sensor surface to overcome fluid forces.[33] Recently, silicon nitride microengineered membranes, also known as microsieves, have been presented as novel detection devices for microorganisms, which are captured on the microsieve whose pore size is smaller than the microorganisms.[34] This method allows for the easy passage of other smaller components while avoiding the limitation of cell diffusion toward the surface as compared to planar microarrays. However, such a microsieve-based approach is hampered by fouling issues and the nonspecific adsorption of undesired components from the processing of crude biological samples. Moreover, the use of a blocking solution before incubation with bacterial solution still is an essential step in minimizing the nonspecific adsorption of proteins, which otherwise leads to interfering background fluorescence. It is advantageous if the use of a blocking solution can be avoided because of associated material and handling issues. Previously, we presented a method to graft zwitterionic polymer brushes from Si_xN_4 surfaces via surface-initiated controlled atom-transfer radical polymerization (ATRP).[27] The grafted polymers displayed excellent protein repulsion and proved to be very stable during prolonged exposure to phosphate-buffered saline (PBS). To reduce nonspecific adsorption on antibody-based biosensor chips, for the current work we decided to immobilize antibodies covalently onto surface-bound protein-repellent zwitterionic polymers. This should provide two advantages: (1) the zwitterionic polymer brushes are grafted from the Si_xN_4 surface via stable Si−C and N−C linkages[27,31,35−37] as compared to less-stable Si−O−Si−C[15,29] and Si−O−C[13,14] linkages; (2) immobilization is facile because of the use of the Br moieties that are retained at the end of the zwitterionic polymer chain after ATRP. As a result, the long-term protein-repellent properties of the zwitterionic polymer should remain largely unaffected.

In this work, we thus present a method to immobilize antibodies onto zwitterionic polymers grafted from Si_xN_4 surfaces and evaluate the sensing properties of the modified surfaces in the specific case of *Salmonella* detection. Sulfobetaine methacrylate (SBMA) zwitterionic polymer brushes were grafted from Si_xN_4 surfaces by controlled surface-initiated ATRP. The zwitterionic polymers were biofunctionalized with anti-*Salmonella* antibodies via the reaction of the primary amine residues on the antibody with NHS moieties attached to the polymers (Scheme 1). The modified surfaces were characterized by X-ray photoelectron spectroscopy (XPS), atomic force microscopy (AFM), and water contact angle measurements. The interactivity of the immobilized antibodies was evaluated by the fluorescence-based detection of SYTO9-labeled *Salmonella* from biological solutions without the aid of a blocking solution.

2. EXPERIMENTAL SECTION

2.1. Materials. 1,2-Epoxy-9-decene (96%), acetone (semiconductor grade), anhydrous dichloromethane, ethylene diamine (99.5%), tris(2-aminoethyl)amine (96%), 4-dimethylaminopyridine (>99%), suberic acid

dx.doi.org/10.1021/la2031363 |*Langmuir* 2012, 28, 604–610

bis(*N*-hydroxysuccinimide ester) (95%), [2-(methacryloyloxy)ethyl] dimethyl-(3-sulfopropyl)ammonium hydroxide (SBMA) (97%), copper-(I) chloride (99.995%) (CuCl), copper(II) chloride (99.995%) ($CuCl_2$), and 2,2′-bipyridine (99%) (bipy) were purchased from Sigma-Aldrich. CuCl was stored under argon. Analytical reagent grade methanol (99.8%) was purchased from VWR. Hydrofluoric acid (50%) was purchased from Fluka. All experiments used ultrapure water, purified by a Barnstead water purification system, with a resistivity of 18.3 MΩ·cm. FITC-streptavidin, Alexa Fluor 488-labeled fibrinogen, and Alexa Fluor 647-labeled fibrinogen were purchased from Invitrogen (U.S.A.). A PBS solution at pH 7.4 with an ionic strength of 0.2 M was used for subsequent washing steps. Sodium phosphate dibasic (analytical grade, Acros), potassium dihydrogenophosphate (ACS grade, Merck), potassium chloride (pro analysis, Merck), and sodium chloride (puriss., Riedel-de-Haën) were used to prepare the PBS buffer. Protein printing buffer solution (PPB, 2×) was purchased from Arrayit Corporation (U.S.A.). Blocking solution was provided by Innosieve Diagnostics B.V., The Netherlands. Fibrinogen (fraction I from porcine plasma, 78% in protein) was purchased from Sigma-Aldrich. Anti-*Salmonella* antibody and FITC-labeled anti-*Salmonella* antibodies were purchased from KPL Inc. (U.S.A.). Green-fluorescence nucleic acid stain SYTO9 was purchased from Invitrogen (U.K.). *Salmonella enterica enterica* serotype Typhimurium bacteria, ATCC 13311 (*Salmonella*), were incubated in PBS solution.

2.2. X-ray Photoelectron Spectroscopy (XPS). Modified surfaces were characterized by XPS using a JPS-9200 photoelectron spectrometer (JEOL, Japan). High-resolution spectra were obtained under UHV conditions using monochromatic Al Kα X-ray radiation at 12 kV and 20 mA with an analyzer energy pass of 10 eV. All high-resolution spectra were corrected with a linear background before fitting. The data were fitted using a deconvolution by Voigt functions (GL30, as implemented in CasaXPS).

2.3. Static Water Contact Angle Measurements. The wettability of the modified surfaces was determined by automated static water contact angle measurements with the use of a Krüss DSA 100 goniometer. (The volume of a drop of demineralized water is 2.5 μL.)

2.4. Atomic Force Microscopy (AFM) for Thickness Measurements. AFM surface images were measured with Tap300Al-G silicon cantilevers (Budgetsensors) in ac mode in air using an Asylum Research MFP-3D SA AFM. Prior to the thickness measurements, the polymer-coated surfaces were immersed in pure water for 4 h at room temperature to swell the polymer fully. A sharp knife was used to scratch the surfaces. The scratched surfaces were sonicated to remove the residuals from cutting, and the sample surface was subsequently dried with argon. The scratched surfaces were directly measured by AFM. The thickness of the swollen polymer layer was determined from the height difference in the topography profile. The thickness obtained by this method was similar to that obtained by ellipsometry measurements. For instance, the polySBMA thickness of 33 ± 2 nm was found to be the same with both methods.

2.5. Confocal Laser Scanning Microscopy (CLSM). Fluorescent images were measured with a confocal laser scanning microscope (Zeiss LSM 510 Meta). Dyes fluorescein isothiocyanate (FITC) and Alexa Fluor 488 were excited with an argon ion laser at 488 nm, and the emission was measured with a long-pass filter with a cutoff wavelength of 530 nm. Alexa Fluor 647 was excited with a He−Ne laser at 633 nm, and the emission was measured with a long-pass filter with a cutoff wavelength of 650 nm.

2.6. Attachment of ATRP Initiators to the Si_xN_4 Surface. Si_xN_4 ($x > 3$) was deposited on Si(100) substrates (p-type, slightly boron-doped, resistivity 8−22 Ω·cm) by LPCVD with a thickness of 150 nm (Nanosens B.V., The Netherlands). The Si_xN_4 wafers were cut into appropriate sizes for each experiment. ATRP initiators were attached to Si_xN_4 through stable Si−C linkages via three consecutive reactions as described previously.[27] In brief, the UV-induced reaction of 1,2-epoxy-9-decene with hydrogen-terminated Si_xN_4 surfaces was followed by the conversion of the epoxide with 1,2-ethylenediamine, resulting in primary and secondary amine-terminated surfaces. Reaction with α-bromoisobutyryl bromide led to ATRP-initiator-coated surfaces.

2.7. Surface-Initiated Polymerization. [2-(Methacryloyloxy) ethyl]dimethyl-(3-sulfopropyl)ammonium hydroxide (SBMA, 4.90 g, 17.5 mmol) and 2,2′-bipyridine (0.14 g, 0.90 mmol) were dissolved in a mixture of methanol (4.0 mL) and water (16.0 mL) in a round-bottomed flask by stirring. The solution was degassed for 30 min by purging with argon. A mixture of CuCl (36.0 mg, 0.36 mmol) and $CuCl_2$ (4.8 mg, 0.036 mmol) was added to a separate round-bottomed flask under argon (in a glovebox), which was closed with a rubber septum. Subsequently, the degassed solution was transferred to a flask containing a mixture of CuCl and $CuCl_2$ by means of a syringe (flushed with argon in advance). The mixture was stirred for an additional 30 min under argon to dissolve all CuCl and $CuCl_2$. Afterward, the mixture was transferred to a reaction flask containing the initiator-coated Si_xN_4 surface by means of a syringe (argon flushed). Polymerization was carried out under argon pressure (0.14 bar overpressure) with stirring at room temperature for a period of time. The samples were removed and rinsed with warm water (60−65 °C) for 5 min, cleaned by sonication in water, and dried under a stream of argon.

PolySBMA-coated surfaces with different thicknesses were prepared with a special holder equipped with a magnet, by which the holder can be moved with an external magnet. The degassed polymerization solution prepared as described above was injected into the reaction flask containing the initiator-coated Si_xN_4 surface. Subsequently, the sample holder was submerged partially in the polymerization solution and moved in further in a stepwise manner at several intervals. The polymerization was carried out under argon pressure with agitation. Finally, the samples were removed and the same cleaning procedure was employed as described earlier.

2.8. NHS-Terminated PolySBMA Surfaces. The polySBMA-coated Si_xN_4 surfaces were further functionalized in two steps. First, polySBMA-coated Si_xN_4 surfaces were reacted with neat tris-(2-aminoethyl)-amine at 45 °C under argon for 6 h to obtain amine-terminated polySBMA (NH_2-polySBMA) Si_xN_4 surfaces. The surfaces were then washed thoroughly with pure water, followed by acetone, and dried under a stream of argon. Subsequently, the surfaces were immersed into a solution of bifunctional suberic acid bis(*N*-hydroxysuccinimide ester) (8.6 mmol·L^{-1}) and DMAP (0.98 mol·L^{-1}) in anhydrous dichloromethane under argon for 18 h.[15] The obtained NHS-terminated polySBMA (NHS-polySBMA) Si_xN_4 surfaces were washed with dichloromethane three times and dried under a stream of argon.

2.9. Attachment of Streptavidin to PolySBMA Surfaces. To evaluate the reactivity of NHS-terminated polySBMA-coated Si_xN_4 surfaces, FITC-streptavidin conjugates were attached to the surfaces. NHS-terminated polySBMA-coated Si_xN_4 surfaces were immersed in fluorescein isothiocyanate (FITC)-labeled streptavidin solution (0.5 mg·mL^{-1} in PBS) at room temperature for 30 min. The surfaces were rinsed thoroughly with PBS before confocal laser scanning microscopy (CLSM) measurements were made.

2.10. Attachment of Antibodies to Modified Si_xN_4 Surfaces. Epoxide-coated Si_xN_4 surfaces[27] were completely covered with antibody solution at a concentration of 1 mg·mL^{-1} in 0.5× protein printing buffer. After incubation for 10 min at ambient temperature, the surfaces were stored at 5 °C overnight. The samples were rinsed three times with PBS solution prior to *Salmonella* detection experiments.[38]

The freshly prepared NHS-terminated polySBMA-coated Si_xN_4 surfaces were incubated with antibody solution at a concentration of 1 mg·mL^{-1} in 0.5× protein printing buffer at room temperature for 30 min. The samples were rinsed three times with PBS solution prior to *Salmonella* detection experiments.

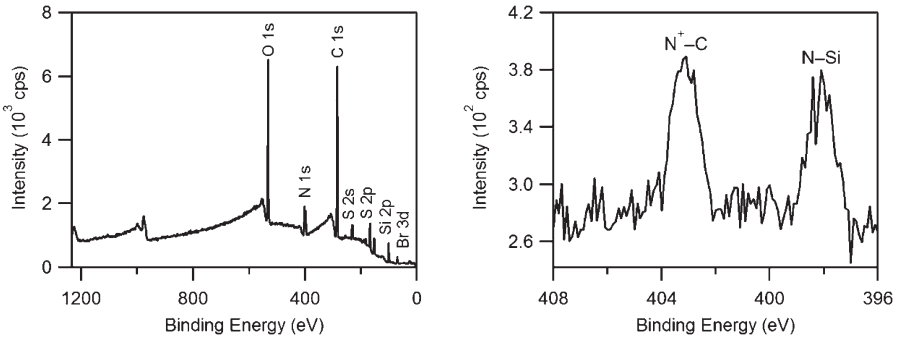

Figure 1. Wide-scan XPS spectrum of the polySBMA-grafted Si_xN_4 surface (left) and narrow-scan XPS spectrum of the N 1s region (right).

2.11. Protein Adsorption. The adsorption of proteins onto zwitterionic polymer-coated surfaces was evaluated by in situ reflectometry using fibrinogen (FIB) solution (0.1 g·L^{-1} in PBS). All reflectometry experiments were performed at room temperature. Before measurements were made, surfaces were incubated for 1 h in warm water (60−65 °C) to wet the coatings sufficiently and subsequently in PBS solution for 1 h to avoid artifacts. After the samples were placed in the reflectometer, PBS solution was injected until the output signal remained constant. Each experiment involved at least one adsorption phase in which FIB solutions were added to the surface and one desorption phase in which only buffer was injected. Details of the preparation of FIB solution and the calculation of the amount of adsorbed protein were described previously.[39]

The second method used to study the adsorption of proteins on modified surfaces was fluorescence imaging to observe adsorbed Alexa Fluor 488-labeled FIB. The modified surfaces were immersed in a solution of Alexa Fluor 488-labeled FIB (0.1 g·L^{-1}) for 1 h at room temperature. The samples were subsequently rinsed three times with PBS and dried under a stream or argon before fluorescence imaging.

2.12. Detection of *Salmonella* by Biofunctionalized Zwitterionic Surfaces. Antibody immobilized on Si_xN_4 surfaces (polySBMA-coated and epoxide-coated Si_xN_4 surfaces) and bare (uncoated) surfaces was incubated in SYTO9-stained *Salmonella* solution in 1× PBS for 15 min. Subsequently, the surfaces were rinsed five times with 1× PBS and then dried briefly with argon before CLSM measurements were made.

2.13. Detection of *Salmonella* by Biofunctionalized Zwitterionic Surfaces in a Mixture of FIB and *Salmonella*. Anti-*Salmonella* antibodies were attached to polySBMA-coated and epoxide-coated Si_xN_4 surfaces as described in section 2.10, and these two types of surfaces were incubated in a mixture of Alexa Fluor 647-labeled FIB (0.2 g·L^{-1}) and *Salmonella* (10^7 cfu·mL^{-1}, with the concentration determined by agar plating) for 15 min; uncoated Si_xN_4 surfaces were similarly treated as reference samples. Subsequently, the surfaces were rinsed five times with 1× PBS and incubated with 1× PBS containing 5 μg of FITC-labeled anti-*Salmonella* antibodies in the dark at room temperature for 15 min. After incubation, the surfaces were rinsed five times with 1× PBS and dried briefly with argon before CLSM measurements. For the comparison of fluorescent images, the same settings were used in all measurements.

3. RESULTS AND DISCUSSION

3.1. Surface-Initiated ATRP. Sulfobetaine methacrylate (SBMA) polymer brushes were grafted via controlled ATRP. For this purpose, Si_xN_4 surfaces were covalently functionalized with an epoxide-terminated monolayer that was reacted with ethylene diamine to yield an amine-terminated surface. Subsequently, ATRP initiators were attached via reaction with α-bromoisobutyryl bromide, as described in detail earlier.[27] After polymerization with SBMA, the water contact angles of the polySBMA-modified surfaces were lower than 20°, indicating the presence of a highly polar coating on the surfaces. These results are in agreement with earlier observations for gold and silicon surfaces coated with polySBMA.[40−42] The wide-scan XPS spectrum of the polySBMA-grafted Si_xN_4 surface showed a significant reduction of the Si 2p signal at 102 eV, demonstrating the presence of a thick polymer layer on the substrate (Figure 1, left). The narrow-scan XPS spectrum of the N 1s region revealed two distinct signals for nitrogen, one corresponding to the quaternary ammonium ions of the polySBMA polymer and one stemming from the nitrogen atoms of the Si_xN_4 substrate (Figure 1, right). The peak at 167 eV that represents the sulfonate moieties in the narrow-scan XPS spectrum of the S 2p region further confirmed the presence of polySBMA on the modified surfaces (Figure S1, Supporting Information). Furthermore, the Br 3d narrow-scan spectrum revealed a signal at 70 eV, showing the retention of the bromide end groups after polymerization (Figure S2, Supporting Information). These results demonstrate that polySBMA was grown in a controlled way from the Br-initiator-coated Si_xN_4 surface. However, the intensity of the bromide signal was found to decrease with increasing polymerization time (Figure S2, Supporting Information). This may be attributed to steric hindrance between adjacent polymer chains during polymerization, particularly when grafting from dense initiator-coated surfaces, which causes some Br moieties to reside within the polymer brush rather than at the periphery, with a concomitant decrease in the Br 3d XPS signal. Moreover, the growth of polymers via ATRP is determined by the complex interplay of a number of factors: solvent, catalyst, monomer, and ligand. In particular, controlled ATRP in water is often hampered by the deactivation of the copper catalyst and the fast propagation rate of the polymerization in this medium.[43−45] Competing side reactions during polymerization may thus yield a diminishing fraction of living polymer chains with increasing reaction times.

The ∼15−20 nm thickness of the zwitterionic polymer brushes was previously demonstrated to give the best protein-repellent performance in a blood solution.[46] When aiming for a similar range of polySBMA thicknesses, we investigated the intensity of retained bromides and the thicknesses of the polySBMA layer and their corresponding protein-repellent properties as a function of the reaction time. The protein adsorption measured by in situ reflectometry showed that a 7-nm-thick polySBMA layer adsorbed 1.4 mg·m^{-2} of FIB whereas a 10 nm thickness of polySBMA allowed the adsorption of only 0.5 mg·m^{-2} (i.e., repelling 91% of FIB as compared to the hydrophobic surface, hexadecyl-coated Si_xN_4[27]) while the signal of Br 3d was still mostly retained. The 15 nm thickness of polySBMA yielded 0.1 mg·m^{-2} of FIB adsorption (i.e., repelling 98% of FIB); however, a further reduction in the Br 3d intensity was found by

dx.doi.org/10.1021/la2031363 |*Langmuir* 2012, 28, 604–610

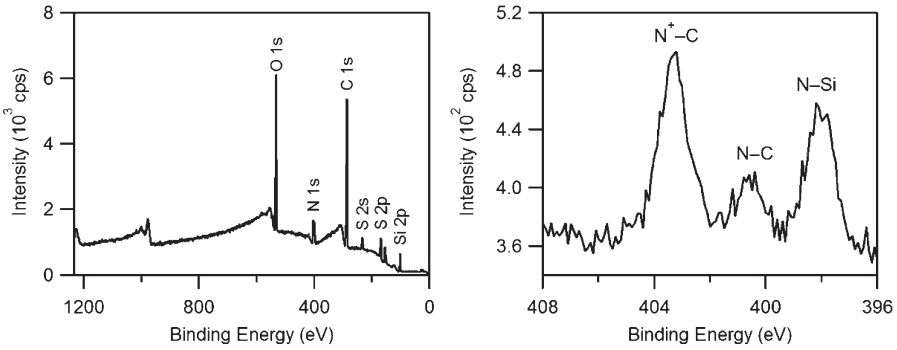

Figure 2. (Left) Wide-scan XPS spectrum and (right) narrow-scan XPS spectra of the N 1s region of the NH_2-polySBMA-coated Si_xN_4 surface.

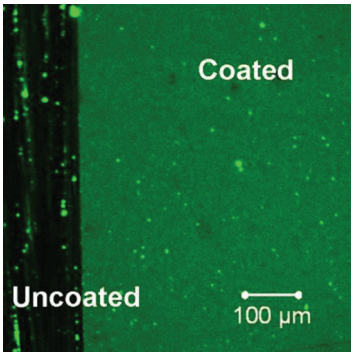

Figure 3. Fluorescent image of a streptavidin-coated zwitterionic coating.

XPS measurement (Figure S3, Supporting Information). To compromise between protein repellence and the number of Br moieties left after polymerization, a thickness of polySBMA of about 10 nm was selected for further functionalization for simultaneous protein repellence and bioselective capture.

3.2. Amine- and NHS-Terminated PolySBMA Brushes. The bromide moieties that were retained at the polymer chain ends may be used for further functionalization as described by Feng and co-workers.[15] The bromides were converted to amine moieties by reaction with neat tris(2-aminoethyl)amine. An additional nitrogen peak appears at 401 eV in the N 1s narrow-scan XPS spectrum (Figure 2, right) between the nitrogen peak stemming from the quaternary ammonium of SBMA and the inorganic nitrogen of the Si_xN_4 substrate. In addition, the signal of Br 3d at 70 eV was no longer observed (Figure 2, left), and the water contact angle remained equally low. This indicates the successful attachment of tris(2-aminoethyl)amine to the polySBMA-coated surfaces to give NH_2-polySBMA Si_xN_4 surfaces.

Following tris(2-aminoethyl)amine attachment, these NH_2-polySBMA Si_xN_4 surfaces were subsequently converted to *N*-hydroxysuccinimide (NHS)-functionalized monolayers by reaction with bifunctional suberic acid bis(*N*-hydroxysuccinimide ester). The water contact angle remained low (typically <20°), indicating the persistence of the hydrophilic polySBMA brush. The integrity of the polymer brush was further confirmed by AFM measurements, which showed that the thickness of the polySBMA film remained constant at 10 ± 2 nm after two consecutive reactions (Figures S5−S7, Supporting Information). Unfortunately, XPS could not be used to follow the reaction progress because the spectra display similar signals for the NHS-functionalized surface as compared to NH_2-polySBMA. Specifically, no significant change was found in the narrow-scan XPS spectrum of the C 1s region, which can be attributed to the overlap of the carbonyl signals of the NHS moieties with the signals of the underlying polySBMA, which are much larger.

3.3. Biofunctionalization on NHS-polySBMA. The attachment of FITC-labeled streptavidin was performed to test the reactivity of the NHS-functionalized surfaces. The fluorescent image displayed a strong FITC signal from the coated area, but the uncoated area (bare Si_xN_4) gave virtually no signal (Figure 3). The fluorescence remained after washing with high-ionic-strength PBS, which shows that a homogeneous surface coverage was obtained for FITC-labeled streptavidin covalently bound to polySBMA-coated Si_xN_4 surfaces. The successful attachment of streptavidin not only demonstrates a high immobilization efficiency of NHS-polySBMA Si_xN_4 surfaces but also opens the way to the immobilization of many biomolecules that have primary amine groups in the side chain onto these protein-repelling surfaces. This procedure was therefore also used for the immobilization of anti-*Salmonella* antibodies. The presence of anti-*Salmonella* antibodies was confirmed by XPS and AFM measurements. The thickness of the modified layer was increased 8 nm after antibody attachment (Figures S8 and S9, Supporting Information). The narrow-scan XPS spectrum of the C 1s region showed a complex mixture of functional carbon groups derived from the chemical composition of the antibody. In addition, the narrow-scan XPS spectrum of the N 1s region showed the disappearance of the inorganic nitrogen peak at 398 eV and the quaternary ammonium nitrogen at 404 eV and a significant increase in the organic nitrogen peak at 400 eV (Figure S10, Supporting Information). These results clearly confirmed the presence of a thick, homogeneous antibody layer on polySBMA after antibody attachment.

3.4. FIB Adsorption on AB-polySBMA Surfaces. The protein-repellent properties of polySBMA-coated Si_xN_4 surfaces after antibody attachment were evaluated by exposure to an Alexa Fluor 488-labeled fibrinogen solution (0.1 $g \cdot L^{-1}$) for 1 h at room temperature and compared to Si_xN_4 surfaces directly coated with antibodies via epoxide chemistry (AB-epoxide)[38] as well as with a bare Si_xN_4 surface. Fluorescent images showed no signal of Alexa Fluor 488 on antibody-coated polySBMA surfaces as compared to the background, but both AB-epoxide and bare Si_xN_4 surfaces displayed strong signals (Figure 4). This observation indicates the nearly complete reduction of the nonspecific adsorption of FIB on AB-polySBMA surfaces, in comparison to

dx.doi.org/10.1021/la2031363 |*Langmuir* 2012, 28, 604–610

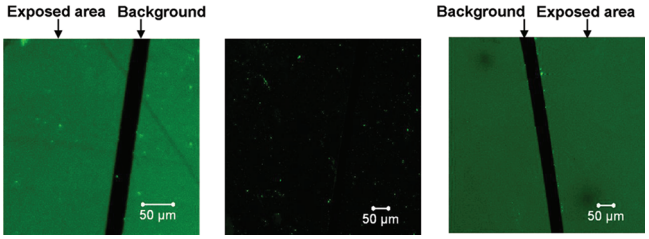

Figure 4. Alexa Fluor 488-labeled FIB adsorbed onto (left) AB-epoxide, (middle) AB-polySBMA, and (right) bare Si_xN_4 surfaces.

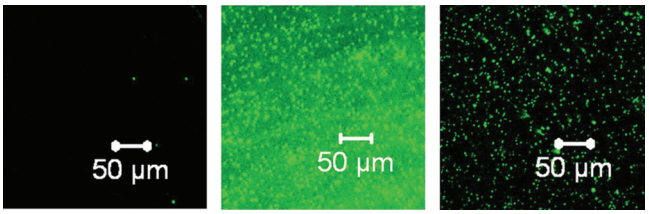

Figure 5. Fluorescent images of (left) bare Si_xN_4, (middle) AB-epoxide, and (right) AB-polySBMA surfaces exposed to *Salmonella* solution without using a blocking solution.

the significant adsorption observed for both AB-epoxide Si_xN_4 and bare Si_xN_4 surfaces.

3.5. Detection of *Salmonella* with AB-polySBMA Surfaces. The binding affinity of anti-*Salmonella* antibodies immobilized on polySBMA-coated Si_xN_4 surfaces was further evaluated by exposure to *Salmonella* bacteria stained with SYTO9 (green-fluorescence nucleic acid stain). The detection performance was compared with that of AB-epoxide and bare Si_xN_4 surfaces and for all of these surfaces without prior use of a blocking solution that would typically contain agents such as bovine serum albumin and Tween-20. The surfaces were incubated with this stained *Salmonella* solution at a concentration of approximately 10^7 cfu. The fluorescent images showed that almost no *Salmonella* was captured on uncoated Si_xN_4 surfaces (Figure 5, left) whereas the AB-epoxide Si_xN_4 surfaces (Figure 5, middle) and AB-polySBMA Si_xN_4 surfaces (Figure 5, right) displayed a significant binding of *Salmonella* with similar fluorescence intensities of the cells. However, the AB-polySBMA Si_xN_4 surfaces had a much lower background signal (high signal-to-noise ratio) as compared to that of AB-epoxide Si_xN_4 surfaces (Figure 5, middle and right). This difference is attributed to the nonspecific binding of either other microorganisms or free DNA present in *Salmonella* solutions, which are also stained with SYTO9 dye as a nucleic acid stain. This attribution is further confirmed by the observation of a lower background for both of the antibody-coated surfaces in the case of using a blocking solution in order to minimize nonspecific adsorption. Interestingly, the amount of detected *Salmonella* on AB-polySBMA surfaces is comparable with that found on antibodies immobilized onto the epoxide-coated Si_xN_4 surfaces. These results show that antibody-functionalized polySBMA surfaces combine excellent protein repellence with the highly efficient capture of *Salmonella* bacteria.

3.6. Detection of *Salmonella* in a Mixture of FIB and *Salmonella*. The protein-repellent and capturing properties of AB-polySBMA were further evaluated by exposing the surfaces to a mixture of Alexa Fluor 647-labeled FIB and *Salmonella* without the prior use of a blocking solution. The detection performance

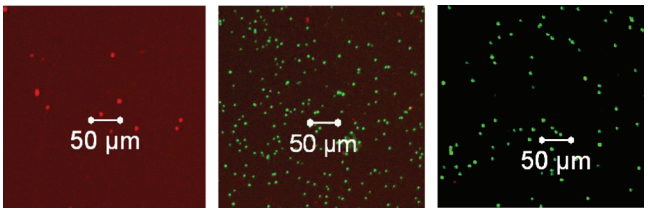

Figure 6. Fluorescence images of (left) bare Si_xN_4, (middle) AB-epoxide surfaces with blocking solution, and (right) AB-polySBMA surfaces without using blocking solution exposed to a mixture of FIB and *Samonella* solution.

and FIB adsorption of AB-polySBMA were compared with those of AB-epoxide surfaces that were treated with a blocking solution beforehand and with bare Si_xN_4 surfaces without using a blocking solution. After exposure to a mixture of the Alexa Fluor 647-labeled FIB and *Salmonella*, the surfaces were incubated with 100 μL of 1× PBS solution containing 5 μg of FITC-labeled anti-*Salmonella* antibodies to visualize the captured *Salmonella* cells. The overlapped fluorescent images of FITC (green) and Alexa Fluor 647 (red) on bare Si_xN_4 surfaces showed only a little attachment of *Salmonella* and the significant adsorption of FIB (Figure 6, left). In contrast, both the AB-epoxide Si_xN_4 surfaces (Figure 6, middle) and AB-polySBMA Si_xN_4 surfaces (Figure 6, right) displayed the binding of *Salmonella*, demonstrating that the attachment of *Salmonella* to these surfaces is specific because of the presence of an antibody. The AB-epoxide Si_xN_4 surface still showed some uniform red fluorescence, indicating a moderate adsorption of FIB on the surfaces, although a blocking solution was used. This can be attributed to the Vroman effect (i.e., FIB can displace earlier adsorbed proteins from the blocking solution) of the surface.[47] In the case of not using the blocking solution, a similar image with a higher intensity of red fluorescence was obtained, indicating the major adsorption of FIB on the surface, which is in agreement with the earlier observation (section 3.4) that the AB-epoxide surfaces adsorbed FIB. Interestingly, AB-polySBMA surfaces (Figure 6, right) showed almost no red fluorescence, indicating virtually no adsorption of FIB onto the surfaces. The result demonstrates that AB-polySBMA-modified surfaces are superior to AB-epoxide-modified surfaces, even when these surfaces are treated with blocking solution to prevent the nonspecific adsorption of proteins during the detection of bacteria in the complex matrices. This highly specific bacterial adsorption of AB-polySBMA in complex media clearly demonstrates the potential of zwitterionic polymer brushes in repelling proteins during bacterial detection.

4. CONCLUSIONS

The coupling of anti-*Salmonella* antibodies to highly stable protein-repellent polySBMA brushes grafted onto Si_xN_4 surfaces yields an antibody-coated surface with a substantial capability for the specific detection of *Salmonella*: even without the blocking solution, *Salmonella* is detected specifically in complex media containing FIB proteins without any detectable FIB adsorption. Such modified surfaces thus present a highly useful platform for the detection of bacteria in crude biological samples. Furthermore, the chemistry involved (surface-initiated ATRP) allows for the attachment of a range of functional moieties to be used at the top of the polymeric layer, demonstrating the wide applicability of such modifiable polySBMA brushes.

dx.doi.org/10.1021/la2031363 |*Langmuir* 2012, 28, 604–610

■ ASSOCIATED CONTENT

Supporting Information. XPS spectra and AFM images of modified surfaces. This material is available free of charge via the Internet at http://pubs.acs.org.

■ AUTHOR INFORMATION

Corresponding Author

*(H.Z.) E-mail: han.zuilhof@wur.nl. Phone: +31-317-482-361. Fax: +31-317-484914. (C.J.M.v.R.) E-mail: cees.vanrijn@wur.nl. Phone: +31-317-482-370. Fax: +31-84-8823204.

■ ACKNOWLEDGMENT

We thank MicroNed (project 6163510587) for financial support, Hien Duy Tong (Nanosens B.V., Zutphen, The Netherlands) for his kind donation of Si_xN_4 wafers, and Ronald van Doorn (Innosieve Diagnostics B.V., Vlijmen, The Netherlands) for assistance during microbial detection experiments.

■ REFERENCES

(1) North, J. R. *Trends Biotechnol.* **1985**, *3*, 180–186.
(2) Kramer, S.; Joos, T. O.; Templin, M. F. *Current Protocols in Protein Science*; John Wiley & Sons: New York, 2005; Chapter 23, Unit 23.5.
(3) Barbee, K. D.; Hsiao, A. P.; Roller, E. E.; Huang, X. H. *Lab Chip* **2010**, *10*, 3084–3093.
(4) Rusmini, F.; Zhong, Z.; Feijen, J. *Biomacromolecules* **2007**, *8*, 1775–1789.
(5) Angenendt, P.; Glökler, J.; Sobek, J.; Lehrach, H.; Cahill, D. J. *J. Chromatogr., A* **2003**, *1009*, 97–104.
(6) Rebeski, D. E.; Winger, E. M.; Shin, Y.-K.; Lelenta, M.; Robinson, M. M.; Varecka, R.; Crowther, J. R. *J. Immunol. Methods* **1999**, *226*, 85–92.
(7) Seurynck-Servoss, S. L.; White, A. M.; Baird, C. L.; Rodland, K. D.; Zangar, R. C. *Anal. Biochem.* **2007**, *371*, 105–115.
(8) Desai, T. A.; Hansford, D. J.; Leoni, L.; Essenpreis, M.; Ferrari, M. *Biosens. Bioelectron.* **2000**, *15*, 453–462.
(9) Mandrusov, E.; Puszkin, E.; Vroman, L.; Leonard, E. F. *ASAIO J.* **1996**, *42*, M506–513.
(10) Sampedro, M. F.; Patel, R. *Infect. Dis. Clin. North Am.* **2007**, *21*, 785–819.
(11) Turner, R. F. B.; Harrison, D. J.; Rojotte, R. V. *Biomaterials* **1991**, *12*, 361–368.
(12) Jonkheijm, P.; Weinrich, D.; Schröder, H.; Niemeyer, C. M.; Waldmann, H. *Angew. Chem., Int. Ed.* **2008**, *47*, 9618–9647.
(13) Brault, N. D.; Gao, C.; Xue, H.; Piliarik, M.; Homola, J.; Jiang, S.; Yu, Q. *Biosens. Bioelectron.* **2010**, *25*, 2276–2282.
(14) Gao, C.; Li, G.; Xue, H.; Yang, W.; Zhang, F.; Jiang, S. *Biomaterials* **2010**, *31*, 1486–1492.
(15) Yao, Y.; Ma, Y.-Z.; Qin, M.; Ma, X.-J.; Wang, C.; Feng, X.-Z. *Colloids Surf., B* **2008**, *66*, 233–239.
(16) Wolter, A.; Niessner, R.; Seidel, M. *Anal. Chem.* **2007**, *79*, 4529–4537.
(17) Stavis, C.; Clare, T. L.; Butler, J. E.; Radadia, A. D.; Carr, R.; Zeng, H.; King, W. P.; Carlisle, J. A.; Aksimentiev, A.; Bashir, R.; Hamers, R. J. *Proc. Natl. Acad. Sci. U.S.A.* **2011**, *108*, 983–988.
(18) Qin, G.; Cai, C. *Chem. Commun.* **2009**, 5112–4.
(19) Leckband, D.; Sheth, S.; Halperin, A. *J. Biomater. Sci., Polym. Ed.* **1999**, *10*, 1125–1147.
(20) Knop, K.; Hoogenboom, R.; Fischer, D.; Schubert, U. S. *Angew. Chem., Int. Ed.* **2010**, *49*, 6288–6308.
(21) Chang, Y.; Chen, W.-Y.; Yandi, W.; Shih, Y.-J.; Chu, W.-L.; Liu, Y.-L.; Chu, C.-W.; Ruaan, R.-C.; Higuchi, A. *Biomacromolecules* **2009**, *10*, 2092–2100.
(22) Chang, Y.; Liao, S.-C.; Higuchi, A.; Ruaan, R.-C.; Chu, C.-W.; Chen, W.-Y. *Langmuir* **2008**, *24*, 5453–5458.
(23) Cho, W. K.; Kong, B.; Choi, I. S. *Langmuir* **2007**, *23*, 5678–5682.
(24) Holmlin, R. E.; Chen, X.; Chapman, R. G.; Takayama, S.; Whitesides, G. M. *Langmuir* **2001**, *17*, 2841–2850.
(25) Ladd, J.; Zhang, Z.; Chen, S.; Hower, J. C.; Jiang, S. *Biomacromolecules* **2008**, *9*, 1357–1361.
(26) Liu, P.-S.; Chen, Q.; Wu, S.-S.; Shen, J.; Lin, S.-C. *J. Membr. Sci.* **2010**, *350*, 387–394.
(27) Nguyen, A. T.; Baggerman, J.; Paulusse, J. M. J.; van Rijn, C. J. M.; Zuilhof, H. *Langmuir* **2011**, *27*, 2587–2594.
(28) Estephan, Z. G.; Schlenoff, P. S.; Schlenoff, J. B. *Langmuir* **2011**, *27*, 6794–6800.
(29) Kitano, H.; Suzuki, H.; Matsuura, K.; Ohno, K. *Langmuir* **2010**, *26*, 6767–6774.
(30) Menawat, A., Jr; J., H.; Siriwardane, R. *J. Colloid Interface Sci.* **1984**, *101*, 110–119.
(31) Sano, H.; Maeda, H.; Ichii, T.; Murase, K.; Noda, K.; Matsushige, K.; Sugimura, H. *Langmuir* **2009**, *25*, 5516–5525.
(32) Rivas, L. A.; García-Villadangos, M.; Moreno-Paz, M.; Cruz-Gil, P.; Gómez-Elvira, J.; Parro, V. c. *Anal. Chem.* **2008**, *80*, 7970–7979.
(33) Skottrup, P. D.; Nicolaisen, M.; Justesen, A. F. *Biosens. Bioelectron.* **2008**, *24*, 339–348.
(34) van Rijn, C. J. M. *Nano and Micro Engineered Membrane Technology*; Elsevier: Amsterdam, 2004.
(35) Scheres, L.; Arafat, A.; Zuilhof, H. *Langmuir* **2007**, *23*, 8343–8346.
(36) Rosso, M.; Giesbers, M.; Schroën, K.; Zuilhof, H. *Langmuir* **2009**, *26*, 866–872.
(37) Rosso, M.; Giesbers, M.; Arafat, A.; Schroën, K.; Zuilhof, H. *Langmuir* **2009**, *25*, 2172–2180.
(38) Nguyen, A. T. Covalent Functionlization of Silicon Nitride Surfaces for Anti-fouling and Bioselective Capture Purposes. Ph.D. Thesis, Wageningen University, Wageningen, The Netherlands, 2011.
(39) Rosso, M.; Nguyen, A. T.; de Jong, E.; Baggerman, J.; Paulusse, J. M. J.; Giesbers, M.; Fokkink, R. G.; Norde, W.; Schroën, K.; van Rijn, C. J. M.; Zuilhof, H. *ACS Appl. Mater. Interfaces* **2011**, *3*, 697–704.
(40) Cheng, N.; Brown, A. A.; Azzaroni, O.; Huck, W. T. S. *Macromolecules* **2008**, *41*, 6317–6321.
(41) Omar, A.; Andrew, A. B.; Huck, W. T. S. *Angew. Chem., Int. Ed.* **2006**, *45*, 1770–1774.
(42) Rodriguez Emmenegger, C.; Brynda, E.; Riedel, T.; Sedlakova, Z.; Houska, M.; Alles, A. B. *Langmuir* **2009**, *25*, 6328–6333.
(43) Bergenudd, H.; Coullerez, G.; Jonsson, M.; Malmström, E. *Macromolecules* **2009**, *42*, 3302–3308.
(44) Terayama, Y.; Kikuchi, M.; Kobayashi, M.; Takahara, A. *Macromolecules* **2011**, *44*, 104–111.
(45) Tsarevsky, N. V.; Matyjaszewski, K. *Chem. Rev.* **2007**, *107*, 2270–2299.
(46) Yang, W.; Xue, H.; Li, W.; Zhang, J.; Jiang, S. *Langmuir* **2009**, *25*, 11911–11916.
(47) Bamford, C. H.; Cooper, S. L.; Tsurutta, T.; Vroman, L. *The Vroman Effect: Festschrift in Honor of the 75th Birthday of Dr. Leo Vroman*; VSP: Utrecht, The Netherlands, 1992.